Available online at www.sciencedirect.com
SCIENCE DIRECT
Journal of the European Ceramic Society 26 (2006) 2593–2601
www.elsevier.com/locate/jeurceramsoc

Biomimetic Mg- and Mg,CO_3-substituted hydroxyapatites: synthesis characterization and in vitro behaviour

Elena Landi [a,*], Anna Tampieri [a], Monica Mattioli-Belmonte [b], Giancarlo Celotti [a], Monica Sandri [a], Antonio Gigante [c], Paola Fava [b], Graziella Biagini [b]

[a] *ISTEC-CNR, Institute of Science and Technology for Ceramics—National Research Council, via Granarolo 64, 48018 Faenza (RA), Italy*
[b] *Istituto di Morfologia Umana Normale, Università Politecnica delle Marche, via Tronto 10/A, 60020 Ancona, Italy*
[c] *Dipartimento di Patologia Molecolare e Terapie Innovative, Università Politecnica delle Marche, via Tronto 10/A, 60020 Ancona, Italy*

Received 3 April 2005; received in revised form 16 June 2005; accepted 18 June 2005
Available online 22 August 2005

Abstract

The doping of the apatite with carbonate or/and Mg ions in biologically-like amounts (6 and 1 wt.%, respectively) was performed. Chemico-physical characterizations and cell culture tests were carried out onto the synthetic Mg- and Mg,CO_3-substituted (~30–40 nm particle size) powders in comparison with stoichiometric HA (~160 nm particle size) to determine as mesenchymal stem cells (MSCs) can directly use the mineral microenvironment to stimulate their own proliferation and differentiation activities. At the same time the growth of human osteoblast like cells (MG-63) was evaluated to determine the compatibility of the synthetic doped apatites for bone substitution. Cell morphology analysis by SEM as well as MTT and ALP tests were performed.

The peculiar chemico-physical properties of the doped (Mg- and Mg,CO_3-substituted) materials improved the behaviours of MSC and MG-63 cells in term of adhesion, proliferation and metabolic activation compared to stoichiometric HA.
© 2005 Elsevier Ltd. All rights reserved.

Keywords: Powders-chemical preparation; Biomimetic materials; Apatite; Biomedical applications

1. Introduction

The synthesis of new substituting materials mimicking natural bone, as an alternative to autograft and allograft bone replacements, still remains one of the most interesting objective of the technological research. Much attention has been recently devoted to the development of new biomimetic non-stoichiometric apatites, which can assure higher rate of biodegradability and bioactivity compared to stoichiometric hydroxyapatite, as consequence of a better comprehension of the functional role of the active groups contained in the natural bone tissue.

A controlled bioreabsorbability is a very important feature in the development of these new materials. Two parameters substantially influence the solubility of hydroxyapatite at physiological conditions: the crystallinity grade of powders and the addition of doping groups which substitute those present in the apatite, in order to make it comparable to that of natural bone tissues. The preparation of low grade crystallinity powders can be realised acting on the physical parameters (temperature, ageing time, etc.) of the synthesis process and/or performing particular chemical dopings. Considering the anionic substitutes, the CO_3^{2-} content of the natural apatites amounts to ~3–8 wt.%[1] depending on the species and on the age of the individual. Not only the total amount but also the position in which the carbonate group enters in the crystalline structure of the apatite is variable, with higher content of B type (CO_3^{2-} group substituting in PO_4^{3-} sites) in respect to A-type (CO_3^{2-} group substituting in OH^- sites) in young bone.[2] Considering the cationic substitutes, Mg ion is quantitatively the most important, amounting typically around 6 mol.%, even if Mg content in the natural apatite is affected by a great variability depending

* Corresponding author. Tel.: +39 0546 699758; fax: +39 0546 46381.
E-mail address: elena@istec.cnr.it (E. Landi).

0955-2219/$ – see front matter © 2005 Elsevier Ltd. All rights reserved.
doi:10.1016/j.jeurceramsoc.2005.06.040

on aging: it is contained in high concentrations in cartilage and natural bone tissue during the initial phases of osteogenesis while it tends to disappear when the bone is mature.[3] In agreement with this finding, Mg ion was found to cause the acceleration of the nucleation kinetics of hydroxyapatite and to inhibit its crystallization process.[4–6] Considering that magnesium depletion adversely affects all stages of skeletal metabolism, causing cessation of bone growth, decrease of osteoblastic and osteoclastic activities, osteopenia and bone fragility, the incorporation of magnesium ions into the hydroxyapatite structure is of great interest for the developing of artificial bone substitutes.[7] It has been suggested [8] that in order to substitute a smaller Mg ion for a larger Ca ion, some additional structural changes may be needed to prevent destabilisation of the structure and subsequent phase decomposition (formation of TCP besides HA) during heat treatment: the co-substitution of a second ionic species and more specifically CO_3^{2-} group is a simple way of achieving this.

Among the works found in literature on the synthesis of Mg- and Mg,CO_3-substituted hydroxyapatite,[4,5,8–16] some are simply based on the immersion of HA or carbonated HA in Mg nitrate solution.[4,8–12] The Mg doping of apatite has been mainly performed using magnesium nitrate as doping source; in the present work Mg chloride (which is otherwise a constituent of the synthetic body fluid) is used as reagent, to synthesise Mg and Mg,CO_3 biological-like substituted hydroxyapatite, starting from the classical neutralisation route involving calcium oxide and ortophosphoric acid. This synthesis allows to avoid additions of ammonia during the process to control and maintain high the value of the pH, contrarily to the synthesis based on calcium nitrate and ammonium hydrogen phosphate, making the whole synthesis easier and more suitable for industrialization. $MgCl_2$ was already used in the synthesis of Mg-doped calcium deficient apatite starting from a mixture of Ca hydrogen phosphate and tetra calcium phosphate powders, both previously synthesized[5]: thus, the interaction among the reactants is not comparable to that involved in our synthesis and it is well known that the physico-chemical properties of the synthetic HA are strongly influenced also by the precursors used. This paper reports also on the co-substitution of Mg and CO_3 in the HA structure by using Na hydrogen carbonate as carbonate source, in order to favour the carbonation in the B-site (phosphate position). The introduction of carbonate ions in the reaction mixture by bubbling carbon dioxide gas was otherwise demonstrated to enhance the contribute of A-site (hydroxyl) carbonation of synthetic Mg substituted hydroxyapatite[8,17,18] giving out carbonated apatites characterized with high A/B carbonation ratio. Mg ions are bivalent as Ca ions, thus the carbonate ion is not 'forced' to substitute in the phosphate site in order to preserve the charge balance, as on the contrary occurs for the Na,CO_3 co-substituted hydroxyapatite, in which the substitution of bivalent Ca^{2+} with monovalent Na^+ stimulates the substitution of trivalent anion PO_4^{3-} with the bivalent anion CO_3^{2-}. The use of Na hydrogen carbonate as carbonate source for the synthesis of Mg,B–CO_3 co-substituted hydroxyapatite appears interesting also considering that Na ions are present in the bone mineral, thus the synthetic product can not be chemically disadvantaged, if Na ion partially enters in the apatite structure.

Finally, investigation of bio-functional performances of human mesenchymal stem cells (MSCs) grown onto these apatitic substrates with different chemical characteristics has been performed, in view of their use in clinics for bone-tissue repair. Human MSCs are multipotent cells present in the adult marrow and are able both to replicate as undifferentiated elements and to differentiate as progenies of the mesenchymal tissue, including bone. In a favourable environment for bone differentiation they realise the expression of an osteoblastic phenotype to reconstruct impaired bone tissue. The MSCs cells show a very short proliferative life span[19] and tend to loose the differentiation potential in the in vitro culture. Moreover, it must be emphasised that MSCs, which are normally present in vivo in the microenvironmental interface between bone and bone marrow, exert sinergic cross-talks with haemopoietic precursors and bone cells and some evidences outline as they, after microenvironmental specific activation can produce both mesenchymal and haemopoietic precursors.[20]

On the basis of these consideration it seems important to determine the in vitro behaviour of mesenchymal stem cells seeded onto an "artificial mineral bone" and also to verify as the MSCs can directly use the mineral microenvironment to stimulate their proliferative–differentiative activities.

Thus, with the aim to realise in the next future hybrid devices that can be easily applied in clinics in association with MSCs to repair bone defects, morpho-functional (MMT and ALP) and scanning electron microscopic (SEM) studies of cells seeded onto three different apatitic substrates were performed. Concomitant bio-functional investigations with a well-studied osteoblast-like cell line (MG-63) commonly used to test in vitro bone-materials biocompatibility were also performed.

2. Materials and methods

2.1. Materials preparation

Stoichiometric hydroxyapatite was prepared, as a control, through the classical neutralization method based on the dropping in 3 h of 600 ml of an aqueous solution containing 88.8 g of H_3PO_4 (Aldrich, 85% pure) into a calcium hydroxide suspension, maintained at 85 °C, prepared dispersing 100 g $Ca(OH)_2$ (Aldrich, 95% pure) into 1000 ml of water. The starting Ca/P molar ratio was therefore equal to the stoichiometric value of hydroxyapatite 1.667. The precipitation product was aged for 24 h at 25 °C, washed and filtered for three times, lyophilised and finally sieved at 150 μm. Mg-doped hydroxyapatite powder (MHA) was similarly prepared dropping the acid solution into the basic suspension

containing 48.4 g of $MgCl_2 \cdot 6H_2O$ (Merck, A.C.S., ISO) and maintained at the temperature of 40 °C. The precipitation product was aged for 24 h at 25 °C washed and filtered for three times, lyophilised and finally sieved at 150 μm. Similarly, the simultaneous doping of the synthetic hydroxyapatite with Mg and carbonate ions (MCHA) was performed including the dropping of 200 ml of 0.8 M $NaHCO_3$ (Merck, A.C.S., ISO) solution into the basic suspension.

2.2. Chemico-physical analysis of the powders

The specific surface area of the powders was evaluated by the Brunauer–Emmett–Teller method (Sorpty 1750, Carlo Erba, Milano, Italy). For particle size distribution measurement, the powders were analysed by sedimentography (Sedigraph 5100, Micromeritics, Norcross, GA) after ultrasonic dispersion for 10 min. The morphological evaluation of the powders was performed by scanning electron microscopy (SEM; Stereoscan 360, Leica, Cambridge, UK). Inductively coupled plasma-optical emission spectrometry (ICP-OES) analysis (Liberty 200, Varian, Clayton South, Australia) and Fourier transformed infrared (FTIR) spectroscopy (Thermo Nicolet-Avatar 320 FTIR) also were performed to determine HA stoichiometry deviations. The elemental analyser (LECO C/S, Leco Corporation, St. Joseph, Michigan, USA) as well as the simultaneous thermal analysis (STA 409 Netzsch Geraetebau GmbH, Selb, Germany) were used to estimate the carbonate amount of the powders. X-ray diffraction (Cu Kα radiation, Miniflex Rigaku, Tokyo Japan) was performed to evaluate the degree of crystallinity, the crystalline phase composition and the carbonation degree of the powders.

2.3. Evaluation of solubility properties

To determine the influence of the ion dopings on the solubility of the powders zeta-potential and conductivity measurements of the powders were carried out with an electroacoustic technique, using an electrokinetic sonic amplitude (ESA) measurement apparatus (Acoustosizer, Colloidal Dynamics, Sydney, Australia). The suspension sample was prepared by ball milling the powder for 1 h into 10^{-2} M KCl solution to maintain a constant ionic strength. The aqueous behaviour of the powders was investigated through potentiometric titration. The isolectric point (IEP) was identified at the pH axis crossing point.

2.4. Isolation and characterisation of MSCs

Bone marrow (BM) was collected from acetabulum and femoral head of two patients (mean age 59 years) undergoing total hip arthroplasty. BM mononuclear cells were obtained by Ficoll (Sigma, Italy) density gradient centrifugation and depleted of $CD45^+$ and glycophorin-A $(GlyA)^+$ cells by means of micromagnetic beads (Miltenyi Biotec, Italy). $CD45^-/GlyA^-$ cells were plated in 75 cm^2 culture flasks (Corning Inc., NY) in mesencult$^+$ stimulatory supplement (both from StemCell, BC) and 1% penicillin–streptomycin (Gibco, Italy) for 14 days. Then near-confluence cultures were processed further by trypsinisation and expansion through sequential passages to confluence. Cells were characterised by FACS Calibur flow cytometry system (Becton Dickinson, CA), using antibodies against the following surface antigens: CD3, CD34, CD14, CD45, CD90 and CD105 (Becton Dickinson, CA).

2.5. Cell cultures

After characterisation MSCs were grown in controlled atmosphere (5% CO_2; $T = 37$ °C) in DMEM (Sigma, Milan, Italy) supplemented with 10% foetal bovine serum (FBS), 1% non-essential amino acids, 2.0 mM L-glutamine, and antibiotics. They were routinely split 1:2 at weekly intervals and used between the 3rd and 4th passages.

MG-63 human osteoblast-like cells (ATCC, Rockville, MD) were grown in identical culture conditions. After thawing, they were routinely split 1:5 every 3–4 days and used between the 3rd and 4th passages.

Cells from confluent MSCs cultures and MG-63 cells were then detached using 0.25% trypsin in 1 mM EDTA and plated in triplicate at a density of 5×10^4 and 1×10^4 cells/cm^2, respectively, onto the different materials to be tested and in 24-well polystyrene tissue culture plates (TCPs) as controls. Culture plates were incubated at 37 °C for 7 days.

2.6. MTT (3-dimethylthiazol-2,5-diphenyltetrazolium bromide) colorimetric assay

After incubation (7 days), the medium was removed; 200 μl of MTT (Aldrich 135038) solution (5 mg/ml in DMEM without phenol red) and 1.8 ml of the medium were added to the cell monolayers; the multi-well plates were incubated at 37 °C for a further 3 h. After discarding the supernatants, the dark blue formazan crystals were dissolved by adding 2 ml of solvent (4% HCl 1N in isopropanol absolute) and quantified spectrophotometrically at 570 nm. The mean and the standard deviation were obtained from sums of three different experiments. The data were analyzed by one-way ANOVA and Bonferroni's test and Student's *t*-test. Statistical significance was tested at $p < 0.05$. The results are reported as percentage over control cultures (TCPs).

2.7. Alkaline phosphatase (ALP) activity

ALP activity was measured by incubating 100 μl of each specimen with 0.5 ml Alkaline Buffer Solution (Sigma 221) and 0.5 ml of Stock Substrate Solution (40 mg *p*-nitrophenyl phosphate disodium, Sigma 104, diluted in 10 ml of distilled water), at 37 °C for 1 h. Production of *p*-nitrophenol in the presence of ALP was measured by monitoring light absorbance by the solution at 410 nm using a spectrophotometer (Secomam, Anthelie light, version 3.8, Contardi, Italy).Each ALP activity was normalized by the cell number.

The mean and the standard deviation were obtained from sums of three different experiments. The data were analyzed by one-way ANOVA and Bonferroni's test and Student's *t*-test. Statistical significance was tested at $p < 0.05$. The results are reported as percentage over control cultures (TCPs).

2.8. Scanning electron microscopy (SEM)

For SEM analysis, culture specimens were fixed in 2% glutaraldehyde in 0.1 M cacodylate buffer (pH 7.4), post-fixed in 1% osmium tetroxide, dehydrated in increasing ethanol concentrations, CPD-dried, mounted on aluminium stubs and gold-sputtered. All specimens were observed with a Philips 505 microscope (Royal Philips Electronic, Eindhoven, The Netherlands).

3. Results and discussion

3.1. Physico-chemical characterization

The physico-chemical characteristics of the synthetic powder are reported in Table 1.

The low temperature of the synthesis and the presence of both carbonate and magnesium ions had a synergic effect making the apatite nuclei smaller and inhibiting the crystallization in the reaction site of the MHA and MCHA powders compared to stoichiometric HA. XRD data showed that all the powders were formed by pure apatitic phase with crystallinity extent Xc (calculated by an experimental method elsewhere reported)[21] lower in the case of simultaneous Mg,CO_3 doping (Fig. 1a–c). SEM analysis of the doped MHA and MCHA powders showed primary particles of about 30–40 nm, that is about 1/4 the particle dimension of synthetic stoichiometric apatite (Fig. 2a and b), and in the range of interest for human tissues.[6] The nanosized primary particles tend to agglomerate, as sedimentography also detected: the particle (agglomerate) size distribution showed the most frequent size and the mean particle size at ≈1–2 μm for both the powders. The density of MHA and MCHA powders, evaluated by helium picnometry, amounted respectively to 2.8 and 2.6 g/cm^3, lower values compared to that (3.16) of stoichiometric HA, as expected as consequence of the ionic substitutions in the hydroxyapatite structure, which in general involve also structure defects (cell distortions, vacancies). The specific surface area values (∼70–90 m^2/g) determined through the BET method are consistent with the nanometric particle size, i.e in accordance with SEM results but respectively about 35–60 times lower than the mean particle size values found by sedimentography.

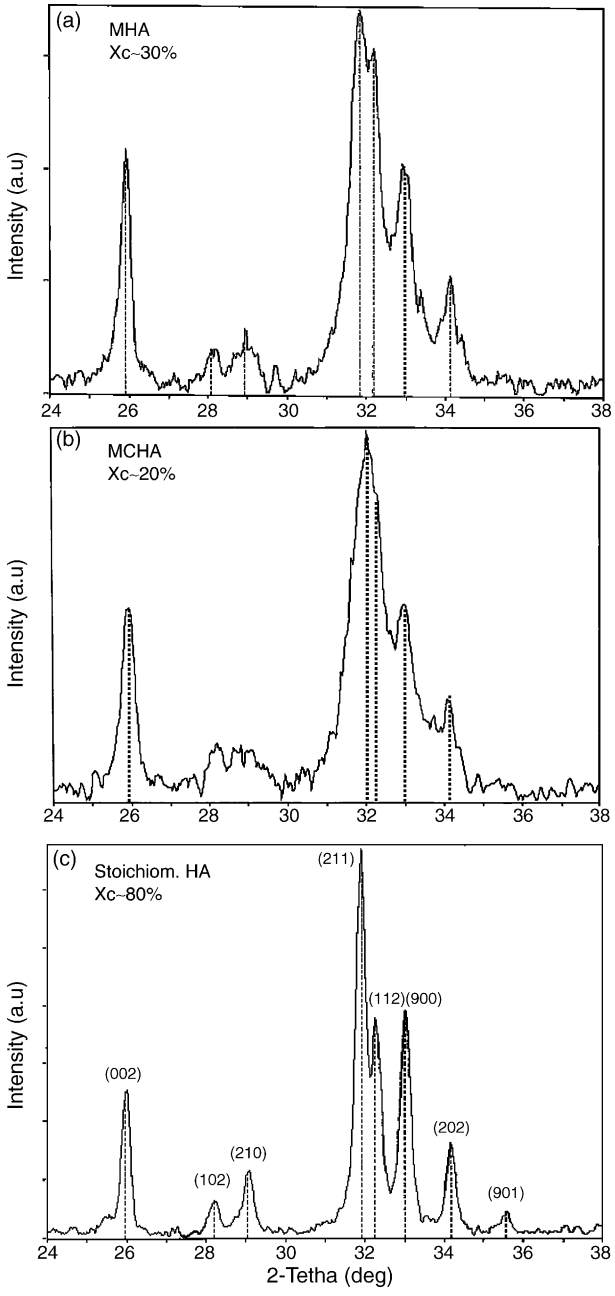

Fig. 1. XRD analysis of: Mg-doped HA powder (a) and Mg,CO_3-doped HA powder (b) compared to stoichiometric HA powder (c).

ICP-AES analysis measured Mg contents in the powders corresponding to ∼30–40% of the total introduced in the starting solutions of the synthesis process, pointing out the

Table 1
Physico-chemical characteristics of the powders

Powder code	s.s.a. (m^2/g)	Xc (%)	Particle size (nm)	$[(Mg + Ca)/P]_{mol}$	$(Mg/Ca)_{mol}$ (%)	B–CO_3 (wt.%)
MHA	∼70	∼40	∼40	∼1.70	∼7	∼2
MCHA	∼90	∼35	∼30	∼1.85	∼7	∼6
HA	∼35	∼80	∼160	∼1.67	–	<0.5

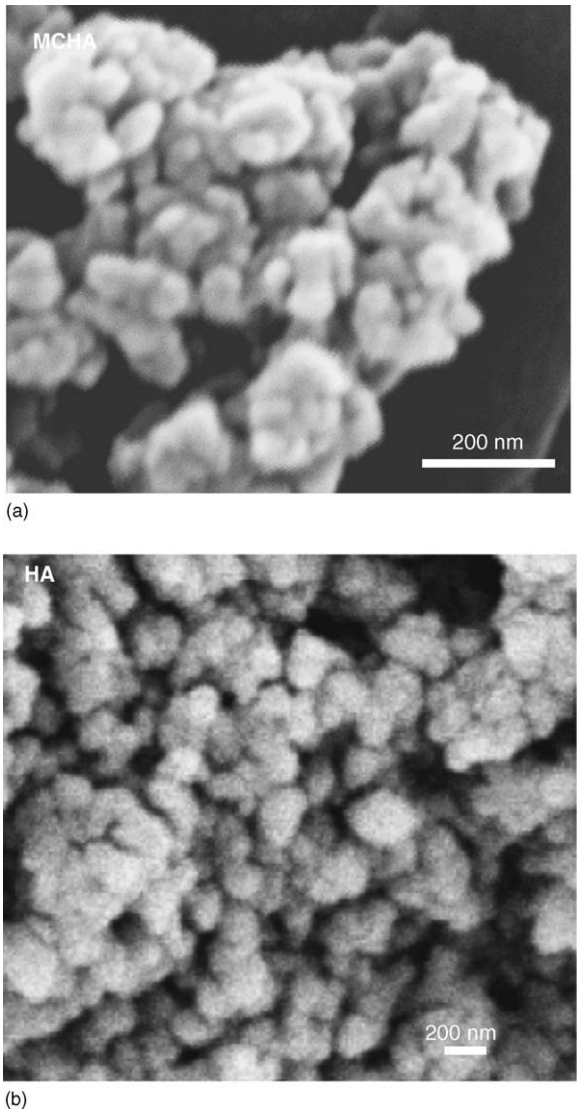

Fig. 2. SEM analysis of: Mg,CO_3-doped HA powder (a) compared to stoichiometric HA powder (b).

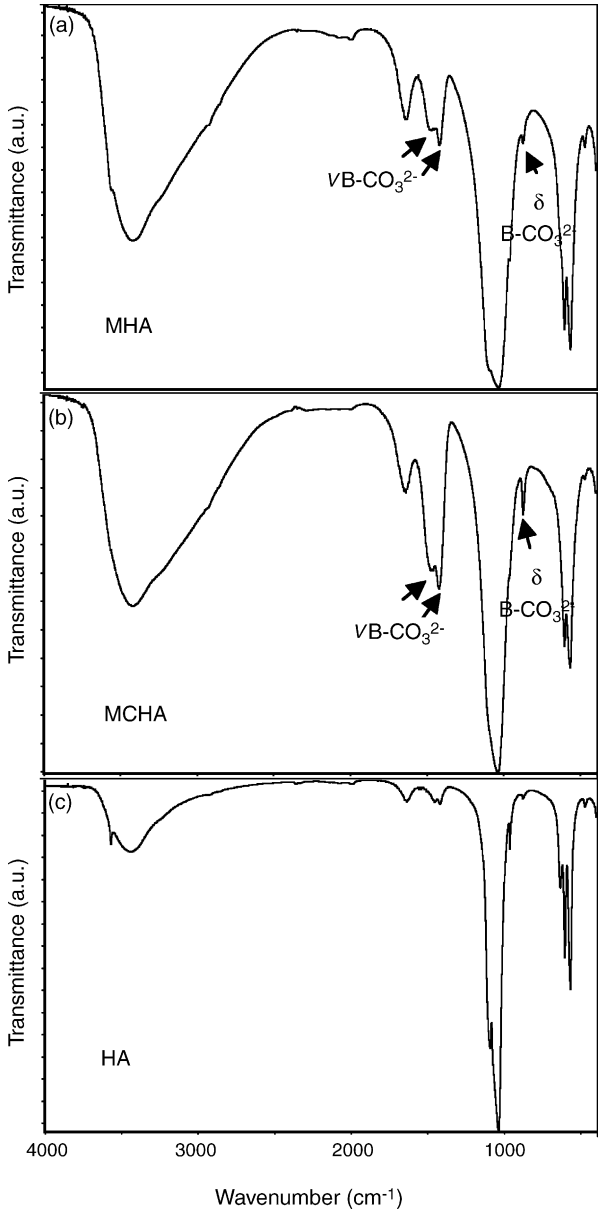

Fig. 3. FTIR analysis of: Mg-doped HA powder (a) and Mg,CO_3-doped HA powder (b) compared to stoichiometric HA powder (c).

realization of a Mg doping ~6.8 mol.% in respect to Ca, corresponding to ~1.2 wt.% of the powder, i.e. close to the Mg biological content. Such doping should be occurred actually as an apatite structural substitution, considering that the maximum possible amount of Mg entering in the apatite structure (~10%)[9,22] was not yet reached and the Mg amount found by ICP-AES was in agreement with the Mg structural value calculated by Rietveld refinements of the XRD data for powders prepared adopting molar Mg cationic fractions in the starting solution up to 0.20[23] (which is higher than 0.16, value concerning the synthesis of this paper and which led to a chemical–structural doping of about 7.5). The (Ca + Mg)/P molar ratio values amounted to ~1.70 and 1.85, respectively for MHA and MCHA. FTIR analysis (Fig. 3a and b) also confirmed the crystallinity trend giving out spectra with broadened profile. Together with the phosphate bands at 980–1100 and 560–600 cm^{-1}, the presence of both the absorbed and the occluded water was detected, being respectively referred to the broad band around 3500 cm^{-1} and to the peak at 1640 cm^{-1}. The FTIR analysis also pointed out (Fig. 3a) that B-type carbonation (substitution in the phosphate site: CO_3^{2-} stretching signals at ~1410 and ~1450 cm^{-1} and bending peak at ~873 cm^{-1}) spontaneously occurred during the MHA synthesis, which was performed without any intentional addition of carbonate source. Such carbonation was due to the carbon dioxide surrounding the reaction vessel, since the synthesis process was intentionally not performed under inert atmosphere. This procedure demonstrated to be effective to realize the spontaneous entering of low carbonate amount in the synthetic hydroxyapatite by simply changing the physical parameters of the synthesis (mainly temperature).[21] By

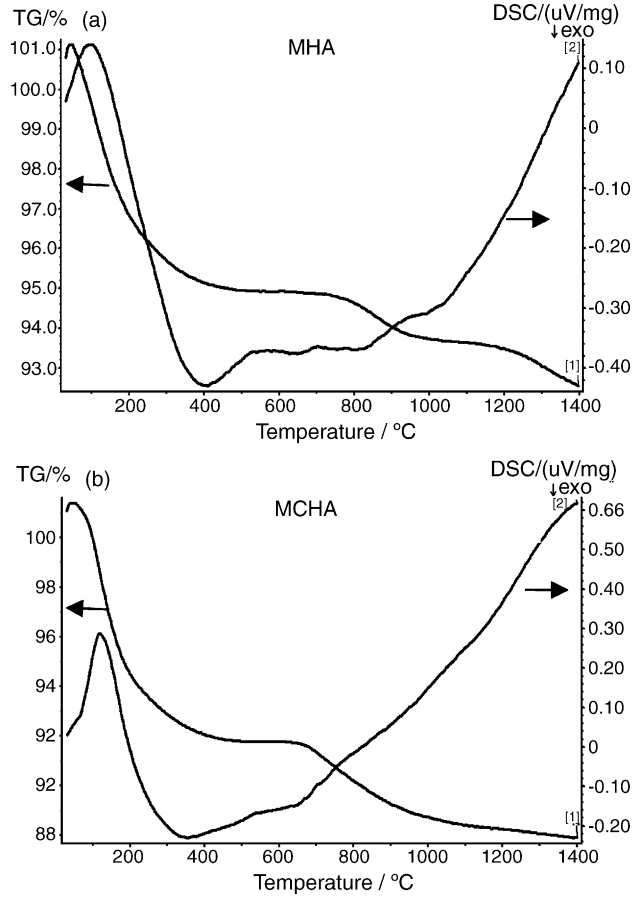

Fig. 4. TG analysis of: Mg-doped HA powder (a) and Mg,CO_3-doped HA powder (b).

thermogravimetric analysis (Fig. 4a), and in agreement with the C elemental analyzer, the spontaneous carbonation was quantified as about 2 wt.% (from the CO_2 weight loss detected in the range 600–1100 °C), which is around the lower limit of the content range of the biological apatite and explains the (Ca + Mg)/P molar ratio ~1.70 found by ICP. For the MCHA powder the TG analysis (Fig. 4b) and the C analyzer estimated a carbonation extent of about 6 wt.%, which the FTIR analysis (Fig. 3b) pointed out to be preferentially in the B site (on the basis of the CO_3^{2-} bending signals at about 880 and 873 cm^{-1}, respectively referring to A-type hydroxyl site and B-type phosphate site). As in the case of MHA, the carbonation extent is responsible for (and in agreement with) the increase of the (Ca + Mg)/P molar ratio from the HA stoichiometric value 1.67 to ~1.85 (value found by ICP for MCHA). The weight loss detected by TGA at high temperature (>1100 °C) is due to the well known dehydroxylation process.

The electrokinetic behaviour of the suspension prepared with the doped powders versus pH was studied and compared with that prepared using stoichiometric HA powder (Fig. 5). The stability range for both MHA and MCHA was shifted towards higher pH values than HAH. The isoelectric point was at higher pH value for the doped apatites (pH ≈ 8.35

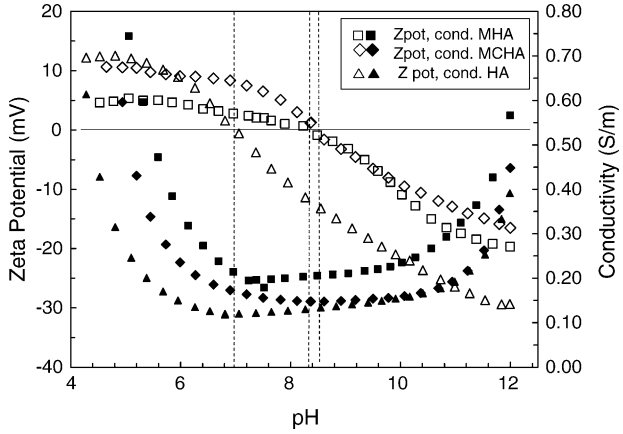

Fig. 5. Electrokinetic behaviour vs. pH of the suspension prepared with the doped powders compared with that of stoichiometric HA powder.

and 8.55 for MHA and MCHA, respectively) with respect to HA (≈6.9). The presence of Mg ion and carbonate group changes the surface behaviour of the powder, giving rise to a higher basic hydrolysis. The analysis pointed out that the MCHA powder was the most soluble, Even if the conductivity value was higher for MHA compared to MCHA. The conductivity is influenced by the surface exposed and by the chemical composition of the powder. Compared to MHA, MCHA even if characterized with higher specific surface area value, tended to more easily agglomerate in suspension at natural pH, thus decreasing the effective surface area exposed and involved in the dissolution phenomenon. Decreasing the pH, the chemical composition becomes an important factor influencing the conductivity: the conductivity curve of MCHA goes up, as consequence of increasing amount of ions in solutions (for decreasing values of pH) starting from higher pH value (pH ≈ 7.6) compared to MHA (pH ≈ 7.2) and HA (pH ≈ 6.7): thus, both the Mg substitution and the B-carbonation improved the solubility of the apatite powder at the physiological pH value (≈7.4).

3.2. In vitro test

In vitro culture showed that the different chemico-physical properties of the powders were able to influence cell behaviour in terms of adhesion, proliferation and metabolic activation. Compared to stoichiometric HA, the MHA and much more MCHA powders represent a suitable substrate, in terms of adhesion and cell proliferation, as for osteoblast-like (MG-63) as well as for osteoblast precursors (MSCs). The results of the MTT test and ALP colorimetric assays of the cells seeded on doped powders (MHA, MCHA) in comparison with those of cells seeded on stoichiometric HA are reported in Table 2.

For MSCs, the MTT values decreased from 88% (MCHA) to 81% (MHA) and to 75% (HA) which was significantly ($p < 0.05$) lower from control cultures. ALP activity was generally low (this can be partially justified because MSCs are stem cells). A significant ($p < 0.05$) reduction in comparison

Table 2
Results of the in vitro test

	MSCs (precursor of osteoblasts)			MG-63 (osteoblastic-like cells)		
	MTT (%)	ALP (%)	Cell shape	MTT (%)	ALP (%)	Cell shape
MCHA	88 ± 8	59 ± 6	Spread	84 ± 7	31 ± 7	Spread
MHA	81 ± 13	64 ± 8	Elongated	86 ± 11	39 ± 6	Intermediate
HA	75 ± 12	63 ± 7	Elongated	70 ± 15	58 ± 5	Spread
CTRL	100 ± 6	100 ± 3	Elongated	100 ± 5	100 ± 4	Spread
Bonferroni *t*-test	CTRL vs. MCHA ns CTRL vs. MHA ns CTRL vs. HA $p<0.05$	CTRL vs. MCHA $p<0.05$ CTRL vs. MHA $p<0.05$ CTRL vs. HA $p<0.05$		CTRL vs. MCHA ns CTRL vs. MHA ns CTRL vs. HA $p<0.05$	CTRL vs. MCHA $p<0.05$ CTRL vs. MHA $p<0.05$ CTRL vs. HA $p<0.05$ HA vs. MCHA $p<0.05$ HA vs. MHA $p<0.05$	

with control culture was detected while no differences between the doped powders and/or the stoichiometric HA were observed.

SEM analysis of cultured cells showed a good compatibility of the MSCs to all the powders tested, even if few cells were observed on the HA granules. In particular, on the MCHA the cells showed a diffuse spread-like morphology with several cytoplasmatic extensions contacting the powder (Fig. 6), while in the case of MHA and HA the cells were elongated with fewer extensions interacting with apatite granules. Control cultures showed a uniform layer of confluent cells with a frequent elongated shape and also overlapping growth (Fig. 7).

As far as MG-63 is concerned, similar viability (MTT values) was observed for cells seeded on both the doped powders (84 and 86%) and these values were both higher (even though not significantly) than the ones (70%) detected on cells seeded on stoichiometric HA powders which resulted significantly ($p<0.05$) lower from control cultures. The enzymatic activity of ALP (either express as IU/L or normalised for cell count) was significantly ($p<0.05$) reduced on all apatite powders in comparison with control cultures. Significantly ($p<0.05$) lower values of ALP activity (normalised for cell count) were detected in cells seeded on doped powders in comparison with those seeded on to stoichiometric HA.

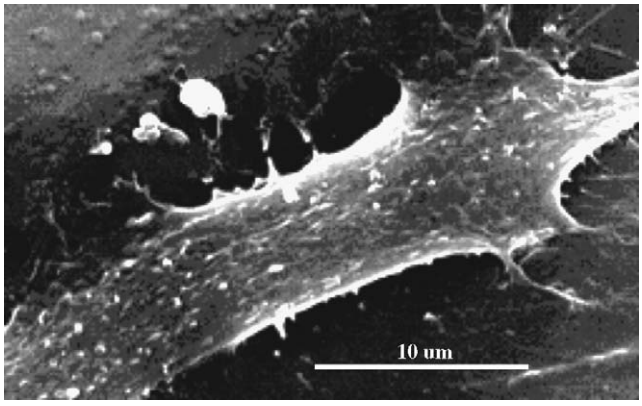

Fig. 7. SEM micrograph of MSCs control culture: confluent cells lying under cells with an elongated shape are present.

SEM observation of culture samples showed a good compatibility of the MG-63 cells with all the apatite powders. On the MCHA substrate, cells with a spread-like morphology with several cytoplasmic extensions contacting the powder (Fig. 8) were observed as for MSCs. Onto the MHA substrate the cell shape was intermediate between elongated and spread, while only spread-like cells were found on the HA

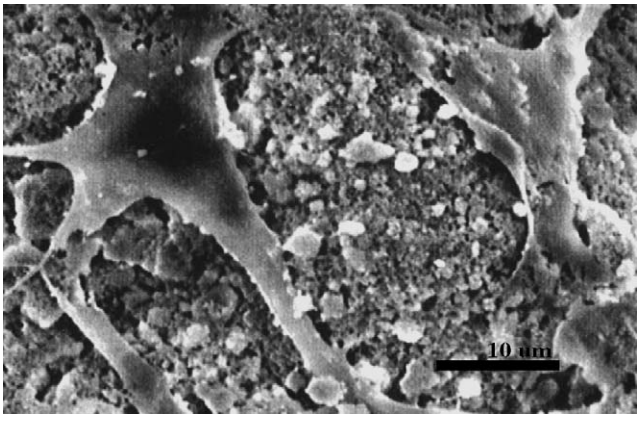

Fig. 6. SEM micrograph of MSCs cultured on MCHA showing cells with a spread-like morphology and cytoplasmatic extensions contacting the powder.

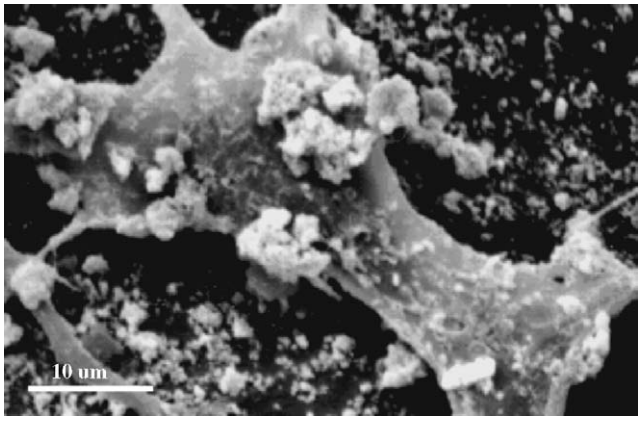

Fig. 8. SEM micrograph of MG-63 cells cultured on MCHA showing several cell cytoplasmic extensions contacting the MCHA powder.

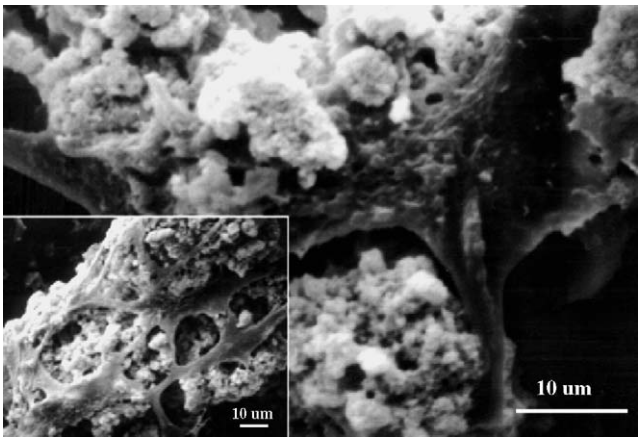

Fig. 9. SEM micrograph of MG-63 cells that tended to anchor to both the MHA and HA substrates, up to form a network, which sometimes wraps completely the apatite substrate (figure inset).

substrate. Anyway, the MG-63 cells tended to anchor to both the MHA and HA, up to form a network, which sometimes wraps completely the apatite substrate (Fig. 9). A monolayer of spread-like cells was observed in control cultures.

The success of bone substitutive materials largely depends upon the formation of mechanically stable and strong interface between materials and bone tissue.[24,25] A series of processes occur through the initial adhesion of cells with bone substitutive materials. Cellular adhesion and subsequent cellular responses on the material are, therefore, critical and prerequisite parameters for osteointegration and osteoconduction.[26] It has already been shown that, although an initial adhesion of the MSCs is lower in HA than in culture plastic, once the cells are adhered, morphology of the cells appears normal.[27] Our morphological analyses could not detect any deleterious morphology of the MSCs grown on the tested materials thus demonstrating good compatibility between cells and substrate even if with a limited ALP expression. These results, which are in line with literature on calcium phosphate cements[27,28] may be at least in part related to acidification of the media subsequent to mineral dissolution or to the absence of further enhancement in the culture media (e.g. β-glycerol-phosphate and L-ascorbic acid-2-phosphate). During differentiation, mesenchymal and osteoprogenitor cells are not particularly sensitive to the type of substrate and they are uniquely affected in their proliferation rate suggesting that cellular response to the type of surface may be strictly related to cell maturation state.[29] As far as MG63 is concerned, MG63 cells which are immortalized, immature and have a high proliferative potential even without any treatment, appear to hold different cross-talks with the different studied powder in comparison with MSCs. Indeed cell culture provides a reductionist's view of cells in a two-dimensional arrangement (in culture dishes) in contrast to their normal-multicellular environment in a three dimensional geometry. However this can be seen as a benefit rather than a disadvantage because it provides with defined experimental settings in which investigating the phenotypic consequences of direct cells/substrate interactions.

The Mg substitution and the Mg,CO_3 co-substitution present several advantages related to metabolic cell behaviours. In fact our results, mainly referred to MSCs (as the continuos line MG-63 is not usable for in vivo therapeutic approaches) evidence as Mg substitution induced a well spread morphology, quite different from the morphology of MSCs grown onto HA (without Mg cationic substitution). The different morphologies observed for MSC and MG63 grown onto the differently doped powder as well as onto stoichiometric HA are difficult to relate directly to FAK enzyme (focal adhesion kinase) activation. In fact, even though FAK are controlled by substrate rigidity as mechanosensor and our differently apatitic substrate display a heterogeneous rigidity, it remains to be determined whether intrinsic FAK catalytic activity or the role of FAK as a scaffolding protein at focal contact is determinant the migration or directional motility.

Finally, technological improvements concerning biological mineralisation allow us to mention a new possible challenge concerning gene-delivery applications. In fact, DNA/mineral nano-composite surfaces (engineered on to cell-culture substrates) with different Ca/P ratio, and containing Mg ions, are able either to support cell growth or provide higher concentration of DNA in the immediate microenvironment of the culture systems. The value of this approach needs to be further tested, but it evidences as the functionalization of mineral matrices can raise new, important medical applications not only related to bone reconstruction.

4. Conclusions

Synthetic HA and ∼6 wt.% carbonated HA both doped with ∼6.5 mol.% (∼1 wt.%) Mg were prepared via wet-chemical synthesis. The chemico-physical characteristics of the doped powders, which are influencing each other, as Mg-doping, B-type CO_3-doping, low crystallinity and high specific surface area, make the synthetic apatite more biological-like and all concur to enhance the solubility of the material at the physiological pH value. The peculiar chemico-physical properties of the doped powders also improved the cell behaviour (MSCs and MG-63) in terms of adhesion, proliferation and metabolic activation, compared to stoichiometric HA. Such improvement was more evident in the case of (1 wt.% Mg + 6 wt.% CO_3) biomimetic co-substituted apatite powder. Moreover, our findings confirm the relevant role of MSCs for the regenerative medicine and for the bone tissue reconstruction.

Acknowledgment

This research work was funded by the European Commission—nmP Programme—nmP3-CT-2003-505711.

References

1. Driessens, F. C. M., *Bioceramics of Calcium Phosphates*. CRC Press, Boca Raton, FL, 1983, pp. 1–32.
2. Rey, C., Renugopalakrishnan, V., Collins, B. and Glimcher, M., Fourier transform infrared spectroscopic study of the carbonate ions in bone mineral during aging. *Calcif. Tissue Int.*, 1991, **49**, 251–258.
3. Bigi, A., Foresti, E., Gregoriani, R., Ripamonti, A., Roveri, N. and Shah, J. S., The role of magnesium on the structure of biological apatite. *Calcif. Tissue Int.*, 1992, **50**, 439–444.
4. Bigi, A., Falini, G., Foresti, E., Gazzano, M., Ripamonti, A. and Roveri, N., Magnesium influence on hydroxyapatite crystallization. *J. Inorg. Biochem.*, 1993, **49**, 69–78.
5. TenHuisen, K. S. and Brown, P. W., Effects of magnesium on the formation of calcium deficient hydroxyapatite from $CaHPO_4{\cdot}2H_2O$ and $Ca_4(PO_4)_2O$. *J. Biomed. Mater. Res.*, 1997, **36**, 306–314.
6. Le Geros, R. Z., Calcium phosphates in oral biology and medicine. In *Monographs in Oral Science*, *Vol. 15*, ed. K. H. Myers. AG Publishers, Basel, 1991, pp. 82–107.
7. Percival, M., Bone health and osteoporosis. *Appl. Nutr. Sci. Rep.*, 1999, **5**, 1–5.
8. Gibson, I. R. and Bonfield, W., Preparation and characterization of magnesium/carbonate co-substituted hydroxyapatites. *J. Mater. Sci. Mater. Med.*, 2002, **13**, 685–693.
9. Bigi, A., Falini, G., Foresti, E., Gazzano, M., Ripamonti, A. and Roveri, N., Rietveld structure refinements of calcium hydroxylapatite containing magnesium. *Acta Cryst.*, 1996, **B52**, 87–92.
10. Correia, R. N., Magalhaes, M. C. F., Marques, P. A. A. P. and Senos, A. M. R., Wet synthesis and characterization of modified hydroxyapatite powders. *J. Mater. Sci. Mater. Med.*, 1996, **7**, 501–505.
11. Fanovich, M. A., Castro, M. S. and Porto Lopez, J. M., Analysis of the microstructural evolution in hydroxyapatite ceramics by electrical characterisation. *Ceram. Int.*, 1999, **25**, 517–522.
12. Bigi, A., Marchetti, F., Ripamonti, A. and Roveri, N., Magnesium and strontium interaction with carbonate-containing hydroxyapatite in aqueous medium. *J. Inorg. Biochem.*, 1981, **15**, 317–327.
13. Baravelli, S., Bigi, A., Ripamonti, A. and Roveri, N., Thermal behavior of bone and synthetic hydroxyapatites submitted to magnesium interaction in aqueous medium. *J. Inorg. Biochem.*, 1984, **20**, 1–12.
14. Ryu, H. S., Hong, K. S., Lee, J. K., Kim, D. J., Lee, J. H., Chang, B. S. *et al.*, Magnesia-doped HA/TCP ceramics and evaluation of their biocompatibility. *Biomaterials*, 2004, **25**, 393–401.
15. Kim, S. R., Lee, J. H., Kim, Y. T., Riu, D. H., Jung, S. J., Lee, Y. J. *et al.*, Synthesis of Si, Mg substituted hydroxyapatites and their sintering behaviours. *Biomaterials*, 2003, **24**, 1389–1398.
16. Fadeev, I. V., Shvorneva, L. I., Barinov, S. M. and Orlovskii, V. P., Synthesis and structure of magnesium-substituted hydroxyapatite. *Inorg. Mater.*, 2003, **39**, 947–950.
17. Landi, E., Tampieri, A., Celotti, G., Vichi, L. and Sandri, M., Influence of synthesis and sintering parameters on the characteristics of carbonate apatite. *Biomaterials*, 2004, **25**, 1763–1770.
18. Gibson, I. R. and Bonfield, W., Novel synthesis and characterisation of an AB-type carbonate-substituted hydroxyapatite. *J. Biomed. Mater. Res.*, 2002, **59**, 697–708.
19. Bruder, S. P., Jaiswal, N. and Haynersworth, S. E., Growth kinetics, self-renewal, and the osteogenic potential of purified human mesenchymal stem cells during extensive subcultivation and following cryopreservation. *J. Cell Biochem.*, 1997, **64**, 278–294.
20. Huss, R. and Moosmann, S., The co-expression of CD117 (c-kit) and osteocalcin in activated bone marrow stem cells in different diseases. *Brit. J. Haemathol.*, 2002, **118**, 305–312.
21. Landi, E., Tampieri, A., Celotti, G. and Sprio, S., Densification behaviour and mechanisms of synthetic hydroxyapatites. *J. Eur. Ceram. Soc.*, 2000, **20**, 2377–2387.
22. Yasukawa, A., Ouchi, S., Kandori, K. and Ishikawa, T., Preparation and characterization of magnesium-calcium hydroxyapatites. *J. Mater. Chem.*, 1996, **6**, 1401–1405.
23. Tampieri, A. C., Landi, E. and Sandri, M., Magnesium doped hydroxyapatite, synthesis and characterization. *Key Eng. Mater.*, 2004, **264–268**, 2051–2054.
24. LeGeros, R. Z., Properties of osteoconductive biomaterials: calcium phosphates. *Clin. Orthop. Rel. Res.*, 2002, **395**, 81–98.
25. Hench, L. L., Bioactive materials: the potential for tissue regeneration. *J. Biomed. Mater. Res.*, 1998, **41**, 511–518.
26. Kieswetter, K., Schwartz, Z., Dean, DD. and Boyan, B. D., The role of implant surface characteristics in the healing of bone. *Crit. Rev. Oral Biol. Med.*, 1996, **7**, 329–345.
27. Deligianni, D. D., Katsala, N. D., Koutsokos, P. G. and Missirilis, Y. F., Effect of surface roughness of hydroxyapatite on human marrow cells adhesion, proliferation, differentiation and detachment strength. *Biomaterials*, 2001, **22**, 87–96.
28. Oreffo, R. O., Driessen, F. C., Planell, J. A. and Triffitt, J. T., Growth and differentiation of human bone marrow osteroprogenitor on novel calcium phosphate cements. *Biomaterials*, 1998, **19**, 1845–1854.
29. Lohmann, C. H., Bonewald, L. F., Sisk, M. A., Sylvia, V. L., Cochran, DL., Dean, D. D. *et al.*, Maturation sates determines the response of osteogenic cells to surface roughness and 1,25-dihydroxyvitamin D3. *J. Bone Miner. Res.*, 2000, **15**(6), 1169–1180.